Investigation of the Effect of Thymoquinone on Egfr/FOXP3 Signaling Pathway in OVCAR3 Human Ovarian Adenocarcinoma Cells

İlhan Özdemir , Ayfer Şanlı Aktaş , Mehmet Cudi Tuncer *

Posted Date: 30 July 2024

doi: 10.20944/preprints202407.2359.v1

Keywords: OVCAR3; Thymoquinone; EGFR; FOXP3; Apoptosis; Metastasis

Article

Investigation of the Effect of Thymoquinone on EGFR/FOXP3 Signaling Pathway in OVCAR3 Human Ovarian Adenocarcinoma Cells

İlhan Özdemir [1], Ayfer Şanli Aktaş [2] and Mehmet Cudi Tuncer [3,*]

[1] Department of Gynecology and Obstetrics, Faculty of Medicine, Atatürk University, Erzurum, Turkey.
[2] Department of Histology and Emryology, Faculty of Medicine, Dicle University, Diyarbakir, Turkey.
[3] Department of Anatomy, Faculty of Medicine, Dicle University, Diyarbakir, Turkey.
* Correspondence: drcudi@hotmail.com; Tel.: +90 412 2488001 (Ext. 4539) (Faculty room), Fax: +90 412 2488440, Mobile phone: +90 532 2744926

Abstract: Aim: In our study, the chemotherapeutic drug doxorubicin (Dox) and the natural anticancer property thymoquinone (TQ) were applied to OVCAR3 human ovarian adenocarcinoma cells and human skin keratinocyte cell line HaCat cells, and their cytotoxic effects were investigated through the EGFR/FOXP3 signaling pathway. Materials and Methods: In our study, different doses of thymoquinone and doxorubicin were applied to the cells for 24, 48 and 72 hours and the cytotoxicity level was determined by the MTT method. With Western blot and qRT-PCR analysis, metastasis markers Epidermal growth factor receptor (EGFR) and forkhead box p3 (FOXP3) and apoptosis marker apoptosis inbibitory 5 (API5) genes and their expression levels were examined. Colony counting was performed after DAPI staining and its effect on cell proliferation was determined. An in vitro wound model for metastasis was created and cell migration was evaluated morphologically. All results were analyzed statistically. Results: By the cell viavility test, it was found that cytotoxicity was at the highest level in the TQ and Dox applied group, metastasis was prevented especially in the TQ and Dox combined treatment group, and by qRT-PCR analysis, the activity in the EGFR and FOXP3 pathway decreased the most with TQ and the amount of protein decreased with TQ and Dox. Conclusion: As a result of the study, it was seen that the highest cytotoxic effect and the highest apoptosis induction occurred with TQ treatment. Additionally, it was determined that a significant decrease in EGFR and FOXP3 levels occurred in TQ and Dox applications.

Keywords: OVCAR3; Thymoquinone; EGFR; FOXP3; Apoptosis; Metastasis

1. Introduction

Ovarian cancer is the deadliest gynecological cancer and it is known that tens of thousands of women die from this cancer every year and it ranks fifth in cancer-related deaths in women [1]. Most women with epithelial ovarian cancer are diagnosed with advanced, metastatic disease characterized by widespread peritoneal carcinomatosis and abdominal ascites [2]. The incidence of death from ovarian cancer can be significantly reduced by developing new methods for early diagnosis and treatment of this fatal disease [3]. Among the treatment methods suggested for ovarian cancer, treatment methods such as surgery and chemotherapy are used [4]. When treatment methods for ovarian cancer are determined and applied, it reoccurs and appears to be resistant to chemotherapy [5]. Generally, cisplatin application in chemotherapy is the most common treatment modality for patients who are resistant in advanced stages [6]. In many cancers, excessive activity due to oncogenic factors leads to loss of activity of suppressor genes in tumors. Therefore, when we consider it as a new approach in cancer, increasing the expression of these genes by turning to genetic and epigenetic factors and playing a positive role in the apoptosis process is of great importance for ovarian and other cancers [7].

 doi:10.20944/preprints202407.2359.v1

Considering the studies carried out in recent years, the increase in studies and information on medicinal plants effective in cancer causes an increase in the treatment methods for cancer types [8]. Studies show that Thymoquinone (TQ), which is seen as an effective weapon especially in cancer, is a product of Nigella sativa, which is a ray of hope in pre-clinical treatments for cancer patients and is known to have anti-tumor activity. Thus, many studies have shown that TQ has numerous molecular mechanisms of action that have been proven to prevent tumor growth and prolong the life of cancer patients. Thymoquinone, known as the main bioactive component of black cumin essential oil, is of great importance in in vitro and in vivo disease models, and has been reported to have promising pharmacological and therapeutic effects in treatment studies [9].

Epidermal Growth Factor Receptor (EGFR) is a transmembrane glycoprotein with an extracellular epidermal growth factor binding domain and an intracellular tyrosine kinase domain that can regulate signaling pathways to control cell proliferation [10]. The EGFR gene is located on chromosome 7p12-13 and belongs to the cell membrane receptor tyrosine kinase family, including EGFR (erbB1), erbB2 (HER2), erbB3 (HER3) and erbB4 (HER4). Among these members of the HER family, EGFR and HER2 are the most frequently altered receptors in cancer [11]. Although EGFR is expressed in up to 90% of certain histotypes of ovarian cancers, this molecule has a response rate of 0-6% in patients with persistent or recurrent disease, preventing it from being a therapeutic target and a potential prognostic biomarker in ovarian cancer [12] and lack of meaningful survival. It provides benefit in patients who respond positively to chemotherapy or whose disease is stable [13].

In our study, we aimed to demonstrate the cytotoxic and antiproliferative effects of thymoquinone, which has antimicrobial, anticancer and anti-inflammatory effects in addition to its antioxidant properties, on OVCAR3 ovarian adenocarcinoma cells on EGFR/FOXP3 and API5 molecules.

2. Materials and Methods

2.1. Cell Culture

The medium used for cell culture in in vitro conditions must contain the substances that the cells need to survive, grow and multiply in in vitro conditions. The medium used in our study is RPMI 1640 medium containing 10% fetal bovine serum (FBS), 1% L-glutamine, penicillin (100 U/ml) + streptomycin (100 µg/ml). The viability, proliferation, passage and follow-up processes of the cells were monitored with an inverted microscope. The cells were incubated in an incubator with 95% humidity and 5% CO2 at 37°C, which is the appropriate culture environment for them, and experiments were started when they reached 80-90% density. Cells were first produced in a T25 flask, multiplied and passaged; They were planted in a T75 flask with RPMI 1640 medium and incubated in an oven at 37°C with 95% humidity and 5% CO2, changing the medium every two days. In order to passage the cells that are monolayers and adhere to them, they must first be removed from the surface to which they adhere. Flasks with 80-90% density were first washed with PBS, thoroughly cleaned of dead cells and cell waste, and then aspirated, then trypsin was added to separate the cells from the flask surface. The cell-medium mixture in the flask was transferred to 15 ml falcons, centrifuged at 1500 g for 4 minutes, and the supernatant was removed. The cells that formed the pellet at the bottom were mixed in 5 ml of medium and planted in the appropriate amount of flasks, and they were incubated to ensure that they adhered to the flask again and proliferated. Cell counting was performed before the cells were removed and added to the flask.

2.2. MTT Assay (Cell Viability) and IC50

TQ and Dox were applied to OVCAR-3 cells at varying doses, and MTT cell proliferation test was performed to determine cell viability in a time- and dose-dependent manner and to determine the dose at which 50% of the cells survive (IC50). The TQ used in the study was provided with 98% purity. MTT "Yellow tetrazolium MTT (3-(4, 5-dimethylthiazolyl-2)-2,5-diphenyltetrazolium bromide)" is a water-soluble substance and turns orange by being reduced to formazone components in living cells. The density of the resulting dye is read on a spectrometer, and cell viability test results

 doi:10.20944/preprints202407.2359.v1

can be quickly evaluated thanks to the formation of formazone, which is proportional to the number of metabolically active cells. Various doses of TQ were dissolved in DMSO at a ratio of 1/1000 in a complete medium with 10% serum, and a 50 mM stock solution was prepared and used. The selected concentration range was determined by taking into account literature information and was carried out according to the test kit protocol. Cells were seeded in a 96-well plate with 5,000 OVCAR-3 cells in each well in 100 µl of growth medium RPMI. The cells were kept in an incubator containing 5% CO2 at 37 °C for 24 hours. At the end of the 24th hour, the medium was aspirated. Then for TQ; working concentrations of 5 µM, 7.5 µM, 10 µM, 25 µM, 50 µM, 75 µM, 100 µM, 250 µM and 500 µM were prepared in complete medium containing 10% FBS. The prepared doses were applied to the wells other than the control wells in 100 µl of broth medium. At the same time, to investigate the time-dependent effect, the same doses were applied for 24, 48 and 72 hours. At the end of 24 hours, 100 µl medium, 50 µl MTT reagent solution A, 1 µl MTT activator solution mixture was prepared for each well and 150 µl was added per well (according to Kit usage). Then, the cells were incubated for 4 hours at 37C in an incubator containing 5% CO2, and the absorbance values of the studied groups were read on the ELISA device at 492, 570 and 650 nm wavelengths. The percentage of cell viability was calculated by dividing the optical density value measured in each well by the control optical density value and multiplying by one hundred to determine the IC50 ratio.

2.3. Wound Healing

The wound healing assay is a method used to measure two-dimensional cell migration. It is based on the creation of an artificial field called a "scratch" on a monolayer of confluent cells, in which cells at the borders move towards the gap to fill the gap, and the movement is observed under the microscope. OVCAR3 cells were seeded in 6-well plates at 2x105 cells in each well. Cells were scraped with a 200 µl pipette tip to create a straight line, symbolizing a wound and aiding in the observation of cell migration. The medium was then removed and the cells were washed with PBS. After washing, serum-free medium containing doxorubucin IC50, thymoquinone IC50 and doxorubicin IC50+thymoquinone IC50 agents was placed at the IC50 values determined in the MTT viability test. In the study, the trial was terminated at the 36th hour, when the wound was 90-100% closed in the control group, and wound healing (cell migration) was photographed in the control and application groups.

2.4. Apoptotic Body Formation

In the project, nuclear morphology changes and apoptotic structures occurring after apoptosis caused by Doxorubicin and Thymoquinone agents were determined in the OVCAR-3 cell line with NucBlue® Live ReadyProbes® Reagent (Thermo Scientific, USA) specific dye. In this context, OVCAR-3 cell lines were planted in 24-well plates at 5x104 cells/well and the cells were incubated at 37 °C and 5% CO2 conditions. The next day, vehicles were applied to these wells and Doxorubicin IC50, Thymoquinone IC50 and Doxorubicin IC50+Thymoquinone IC50 agents were applied using the IC50 values obtained in the 48-hour application. At the end of the application, staining was done directly as live cell staining in accordance with the kit protocol, and the cells were incubated at 37°C for 30 minutes. At the end of this period, the plates were photographed using the Thermo EVOS® FL Imaging System using bright field mode and fluorescence mode and a DAPI filter at 20x objective magnification.

2.5. RNA Isolation

In our study, TQ IC50 and Dox IC50 doses were applied to OVCAR-3 cells for 24, 48, 72 hours and RNA was isolated in order to evaluate expression at the gene level. After RNA isolation, cDNA was produced separately for each TQ and Dox group and RT-PCR was performed. According to RT-PCR results, the most appropriate dose was found to be 48 hours. While determining the dose for TQ and Dox and applying it to the experimental groups after finding the appropriate dose, RNA isolation was performed in order to evaluate expression at the gene level. The concentration and purity of the

 doi:10.20944/preprints202407.2359.v1

isolated RNA were determined with the help of Nanodrop device (Thermo). In measuring RNA samples with Nanodrop, RNA samples must first be at appropriate concentrations (the RNA concentration range that the device can measure is 2-3000 ng/µl). Then, a drop of 1µl RNAse-free water was placed on the Nanodrop device base and blindly taken with the program analysis on the computer (ND1000 V3.6.0). Afterwards, 1 µl of RNA samples were pipetted and readings were made at 260-280 nm. The resulting RNAs can be stored at -20 or -80 in Eppendorf. It was measured on the Nanodrop device at a wavelength of 260-280 and the concentration was measured as ng/µl.

2.6. cDNA Synthesis

For cDNA synthesis from the isolated RNAs, cDNA Synthesis Kit (High Capacity) with Rnase Inhibitor was used, oligo d(T) primer and Reverse Transcriptase enzyme (RT) in accordance with the manufacturer's protocol. It is a sensitive molecular method used for quantification of the gene expression product. With this method, RNA samples can be analyzed qualitatively and quantitatively in a short time, and a large number of samples can be studied. In real-time RT-PCR, the analysis of the products is done during the reaction. Therefore, there is no need for processes such as electrophoresis and imaging of the PCR product under ultraviolet light. In our study, an RT-PCR system capable of reading a 96-well microplate was used. After ALA and TGF ß treatment, the expressions of genes involved in EMT (E-cadherin, vimentin, Snail, Slug, Twist, Zeb) at the RNA level were determined using the relevant cell line. Total RNA was isolated from the cell line, and then the quantity and quality of the RNA obtained were determined. Afterwards, cDNA synthesis was performed from total RNA with cDNA Synthesis Kit (High Capacity) with RNase Inhibitor. With this method, analysis can be performed simultaneously and quantitatively with RT-PCR (Thermo Scientific PikoReal 96). By including reference-housekeeping genes in the PCR control group in each panel, we have the opportunity to analyze the relative change in target genes. Amplicons obtained during PCR were evaluated according to the number of cycles in which they went directly to logarithmic increase. First, a standard amplification curve of GAPDH and other housekeeping genes with known concentrations was created, then the relative amount of cDNA was determined by the quantitation software according to the transition point in the sample studied. The data obtained was recorded as Cq. The primer sequences of the epithelial-mesenchymal transition-related genes analyzed and the housekeeping gene (GAPDH) used in normalization as the reference gene are shown in Table 1.

Table 1. The primer sequences of the epithelial-mesenchymal transition-related genes analyzed and the housekeeping gene (GAPDH).

EGFR: F: GCCAAGGCACGAGTAACAAGC, R: GGGCAATGAGGACATAACC
FOXP3: F: GTGGCCGGATGTGAGAAG, R: GGAGCCCTTGTCGGATGATG
B-Actin: F: CCTCTGAACCCTAAGGCCAAC, R: TGCCACAGGATTCCATACCC
GAPDH: F:CGGAGTCAACGGATTTGGTCGTAT, R:GCCTTCTCCATGGTGGTGAAGAC

2.7. qRT-PCR Analysis

In the study, the expression levels of EGFR and FOXP3 genes responsible for EGFR/FOXP3 signaling pathways in the control and application groups of OVCAR-3 ovarian carcinoma cells were analyzed by qRT-PCR method. The primers used to investigate the changes in the expression of these genes are given below, in 5′-3′ order.

cDNAs obtained from isolated RNAs are used in gene expression studies. These cDNAs were performed in qRT-PCR according to the appropriate protocol called Power Sybeer Green qPCR MasterMix (thermo, USA). In this study, Applied Biosystems QuantStudio 5 Real-Time PCR device was used, thus cDNAs were amplified. As a first step, for the qRT-PCR reaction to occur, step 1: Enzyme activation: 95ºC-10 min; 2nd step: Denaturation: 95ºC-15s; Primer binding-Chain extension: 60ºC-1 min, Step 3: Melting curve: 95ºC-15s, 60ºC-1 min, 95ºC-15s. Ct values of the peaks that emerged during the amplification process were used to identify gene expressions and gene expressions were calculated with the 2-ΔΔCt method. In addition, the calibration process and endogenous control

 doi:10.20944/preprints202407.2359.v1

GAPDH (glyceraldehyde 3-phosphate dehydrogenase) and β-actin mRNA expressions multiple control method is provided as a correction factor.

2.8. Western Blot (EGFR, FOXP3)

In the study, OVCAR-3 cells were planted in 75 cm2 culture flasks and incubated until the logarithmic phase was reached. When the cells reached the logarithmic phase, Vehicle control, Doxorubicin IC50: 2.12 µM, Thymoquinone IC50: 62.9 µM doses were applied individually and in combination. Protein isolation was performed from the samples 48 hours after the application. The medium was removed from the flasks and the collected cells were mixed with 500 µl RIPA lysis buffer, 2 µl PMSF solution, 2 µl sodium orthovanadate solution and 2 µl protease inhibitor (RIPA Lysis Buffer System, sc-24948, Santa Cruz, USA) using a Daihan 15D tissue homogenizer (It was homogenized under cold conditions (27,000 rpm). The homogenate was centrifuged at 14000 x g for 20 min. Protein amounts (approximately 1.2-1.6 mg/ml) were determined by the Protein A280 method using Optizen Nano Q, Mecasys, Korea nano spectrophotometer. Then, proteins were loaded on NuPAGE® Bis-Tris polyacrylamide gel (10%) and electrophoresis was performed. In the study, Western Breze brand ready-made kits provided by Thermo Scientific company were used, and blotting and membrane transfer were carried out using the iBlot 2 (Life Technologies) system, using ready-made membranes and kits, and following the kit protocols. Proteins after blotting Anti- EGFR (Ab-1070) Antibody (ABM, CAT no: Y021073), FOXP3 Antibody [C3], Cterm (GeneTex, CAT no: GTX107737), Beta actin Antibody (Invitrogen, CAT no: MA1-140) were treated with specific primary antibodies, then the antibodies were labeled with appropriate secondaries and observed with the Micro ChemiDoc (DNR Bio-Imaging Systems Ltd., USA) gel imaging system. Band intensities were calculated using GelQuant software.

2.9. Protein-Protein Interaction (PPI) Analysis

PPI data were retrieved from the STRING database. The STRING database provides descriptions of protein-protein interactions (PPIs) as well as confidence intervals for data scores. A confidence score greater than or equal to 0.4 was chosen to construct the interaction network of proteins with target genes.

2.10. Enrichment Analysis

Data on the functional annotation of genes and the canonical pathways associated with the strong connections established with these proteins were obtained using the ShinyGO 0.80 program.

2.11. GO Functional Enrichment Analysis

Three types of Gene Ontologies (GO) were performed on possible target genes: cellular component (CC), biological process (BP) and molecular function (MF). The SRplot bioinformatics program was used to evaluate these data.

2.11. Statistical Analysis

The difference between the averages of cell viabilities determined by the MTT test and expression values obtained from qRT-PCR studies was determined by one-way ANOVA. Comparisons between two groups were determined by the independent sample t test or Mann Whitney U test, depending on the homogeneity of the data. Analyzes were performed with SPSS 20 (IBM, USA) program and $p \leq 0.05$ was used.

3. Results

3.1. MTT Findings

Within the scope of the study, the results obtained by applying MTT test on OVCAR-3 cell series after Doxorubicin applications, % cell viability and IC50 values by calculating with these results

 doi:10.20944/preprints202407.2359.v1

obtained by applying probit analysis, the statistical data when compared to the control are shown. As a result of these data obtained, IC50 value could not be found as a result of 24-hour Dox application to the OVCAR-3 cell line. After 48 hours of Dox application, the IC50 value was found to be 2.12 µM, and after 72 hours of Dox application, the IC50 value was found to be 0.08 µM. It was observed that there were significant decreases in cell proliferation as the dose increased. According to the data of the statistical analysis, after the IC50 value was found, it was determined that the cell viability was significant and decreased significantly after 0.5 µM Dox application compared to the vehicle group (Figure 1).

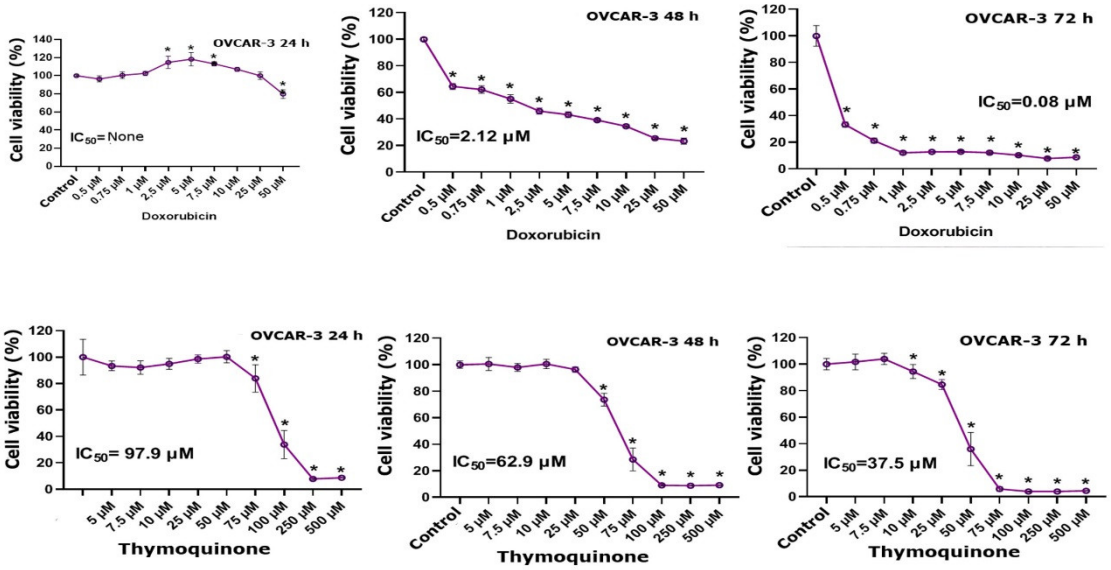

Figure 1. Effect of Dox and 5-500 µM TQ application obtained by serial dilution in the concentration range of 0.5-50 µM in OVCAR-3 cells on % cell viability and IC50 value of the chemotherapy agent compared to the vehicle control group. *data are statistically significant compared to control, one-way ANOVA, Tukey HSD test, p≤ 0.05.

The IC50 value obtained as a result of TQ application to the OVCAR-3 cell line within 24 hours was found to be 97.9 µM. As a result of 48 hours of application, the IC50 value was determined as 62.9 µM and the IC50 value obtained during the 72-hour period was determined as 37.5 µM. After this, one-way ANOVA and Tukey HSD test were used to calculate the statistical significance between the vehicle group and different concentrations of TQ according to $P \leq 0.05$. As a result, it was observed that there was a significant decrease in cell viability after 75 µM concentration with TQ applied for 24 hours, after 50 µM concentration in the 48th hour, and after 25 µM concentration in the 72nd hour (Figure 1).

Dox and TQ were also applied to the healthy cell series and the resulting effect was analyzed, and after the application of both agents, the % cell viability resulting from the MTT test in the HaCaT cell series and the IC50 values calculated using probit analysis will also be included, as well as the statistical analysis obtained when compared to the control. is located. IC50 value could not be obtained by applying Dox to the HaCaT cell line for 24 hours. It was detected as 5.32 µM at the 48th hour and 1.23 µM at the 72nd hour. Thus, it was observed that as the dose increased, significant decreases occurred in cell proliferation (Figure 2).

Preprints.org (www.preprints.org) | NOT PEER-REVIEWED | Posted: 30 July 2024 doi:10.20944/preprints202407.2359.v1

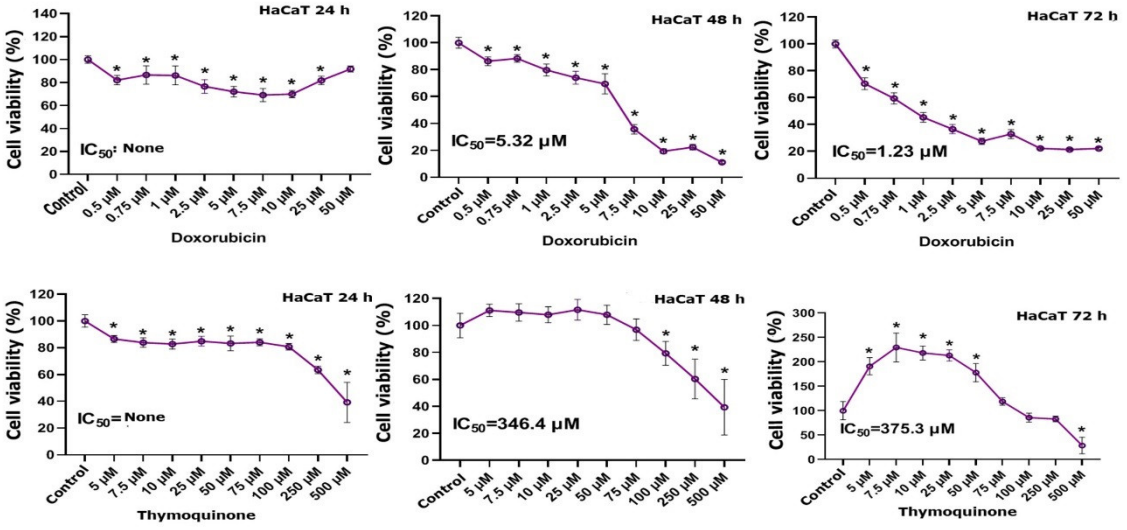

Figure 2. Effect of Dox and 5-500 µM TQ application obtained by serial dilution in the concentration range of 0.5-50 µM on HaCaT cells on % cell viability and IC50 value of the chemotherapy agent compared to the vehicle control group. *data are statistically significant compared to control, one-way ANOVA, Tukey HSD test, p≤ 0.05.

In OVCAR-3 cells, wound closure from the healing test was evaluated at time intervals ranging from 0 to 36 hours. Recovery in OVCAR-3 cells after Dox-TQ application was evaluated by observing the reduction in wound size and cell migration in % compared with the control group t = 0. When the changes in wound sizes were measured, it was seen that the wound size in the control group closed with near 100% cell migration after 36 hours. It was found to drop to 0 µm. In the cells treated with doxorubicin, it was observed that the wound area, which had no cells at 0 hours, was closed with cell migration approaching 50% after 36 hours (Figure 4). In cells treated with thymoquinone, it was observed that the wound area, which was completely open at 0 hours at the beginning of the experiment, attempted to be closed with over 20% cell migration after 36 hours. In the Dox+TQ treatment group, it was determined that cell migration for wound healing remained below 20% after 36 hours. Consistent with these results, it was determined that application of a combination doxorubicin-thymoquinone resulted in lower wound healing than application of Dox and TQ alone in OVCAR-3 cells (Figure 3).

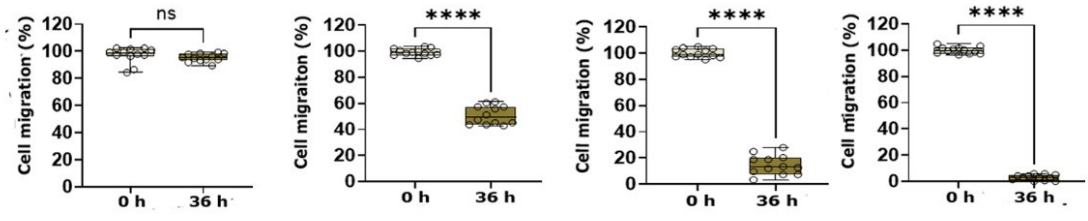

Figure 3. Cell migration rate and statistical significance in the wound healing model.

 doi:10.20944/preprints202407.2359.v1

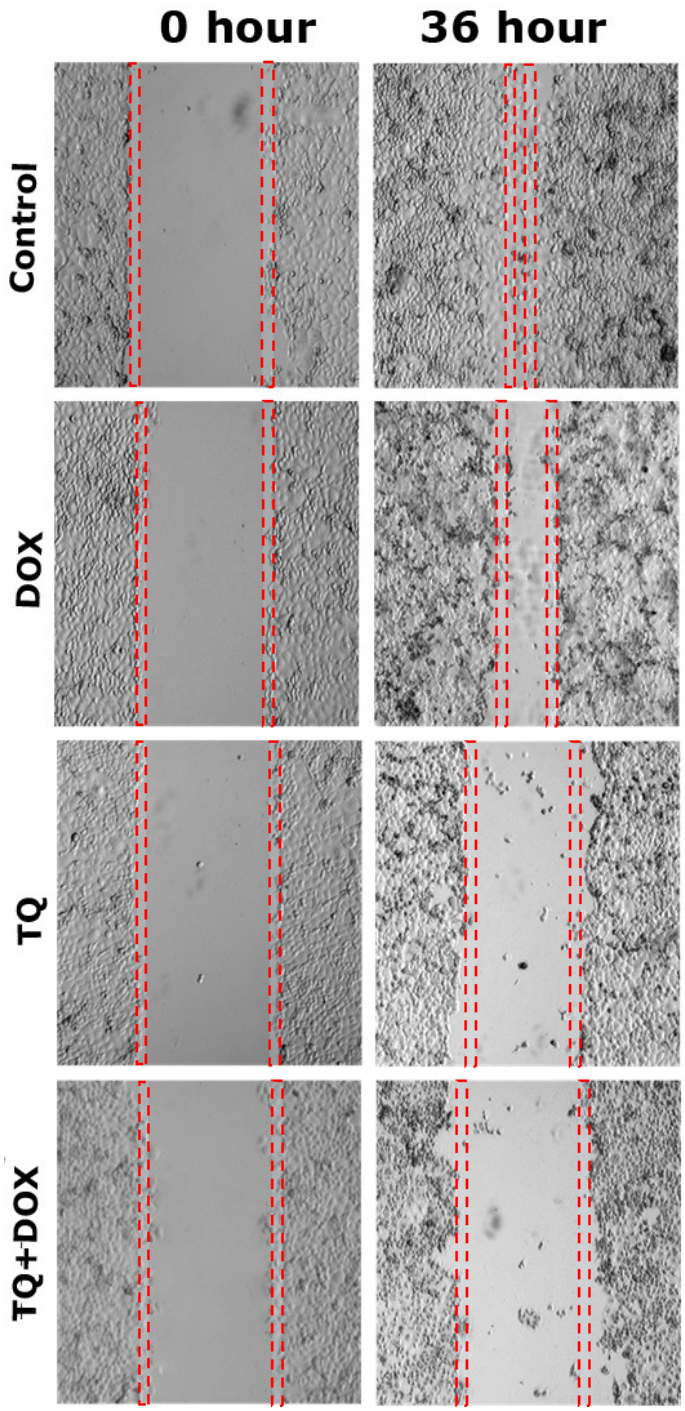

Figure 4. Wound healing assay in OVCAR-3 cell populations treated with vehicle control, Dox IC50: 2.12 μM, TQ IC50: 62.9 μM, and TQ+Dox IC50. N= 12, Bars indicate mean ± Std error; * data are statistically different, calculated using independent samples t-test, $p \leq 0.001$.

3.2. Nucblue Staining Findings

Nucblue staining was performed on all samples treated with TQ and Dox in order to confirm the results of the MTT analysis and to determine whether the cell deaths detected were apoptotic. It was determined that cell death increased in both TQ and Dox applied samples as the application dose increased. After MTT analysis, cell viability was found to be 62.44% and 49.35%, respectively, in cultures treated with 100 μM/L TQ and 1000 nM/L Dox. However, in NucBlue staining, it was determined that cell proliferation was suppressed above these doses and therefore the number of

 doi:10.20944/preprints202407.2359.v1

cells decreased. Increased nuclear fragmentations indicate that apoptosis has occurred. Light microscope images also support this (Figure 5).

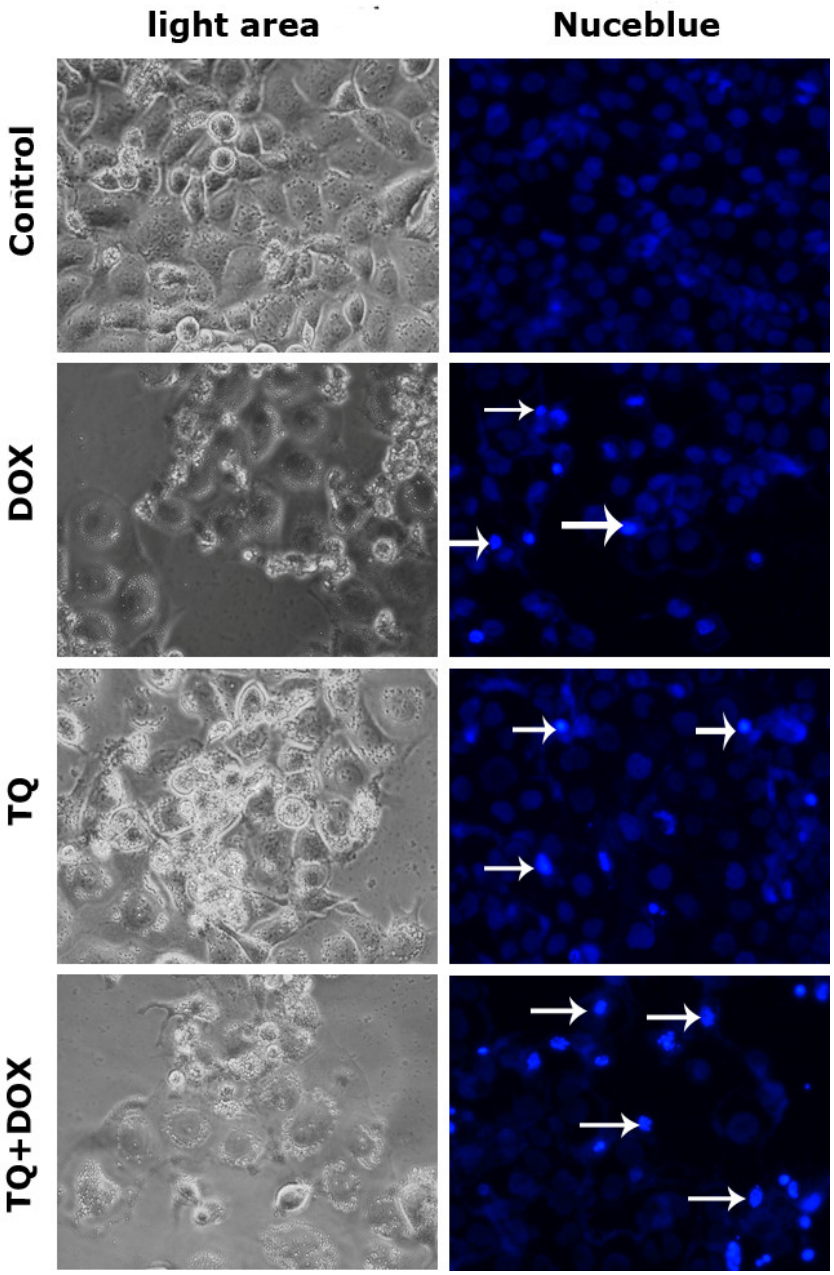

Figure 5. Cell morphology, nuclear structure and apoptotic body formation in OVCAR-3 cell populations treated with IC50 doses of treatment agents for 48 hours. (Arrow: apoptotic cells).

RT-qPCR experiments were performed on a total of 9 samples in all experimental groups; Proapoptotic EGFR and FOXP3 gene expressions were normalized to the β-actin expression of the same sample, which was used as an internal control gene. EFGR, FOXP3 and β-actin gene expressions were determined at detectable levels and amplification curves were created. The amplification curves of these genes were determined with the number of cycles on the x-axis and the Rn value on the y-axis.

As a result of the calculations, EGFR and FOXP3 showed a very high decrease in the 48-hour control group. Although EGFR gene expression was determined at a detectable level in the group where only Dox was applied for 48 hours, no statistical significance could be determined between it and the control group. A statistically significant difference was detected in EGFR gene expression

 doi:10.20944/preprints202407.2359.v1

between the control and TQ+Dox (p=0.0011) and control and TQ+Dox (p=0.035) groups (Figure 6). It was determined that FOXP3 gene expression (RQ=0.5) was expressed at the most significant level in the Dox group, with a decrease of 50%. FOXP3 gene expression in the Dox-treated group showed a statistically significant difference compared to the control and TQ-treated groups. Significance was determined as p<0.0001 between Dox and the control group, and p<0.027 between Dox and TQ. No statistical difference was detected between Dox and Dox+TQ groups. A significant difference was detected in FOXP3 gene expression in the TQ-treated group only between the control and Dox groups. No significance could be detected when compared to other groups. A statistically significant difference was detected in FOXP3 gene expression between the control group and the Dox + TQ group (p = 0.0001) (Figure 6).

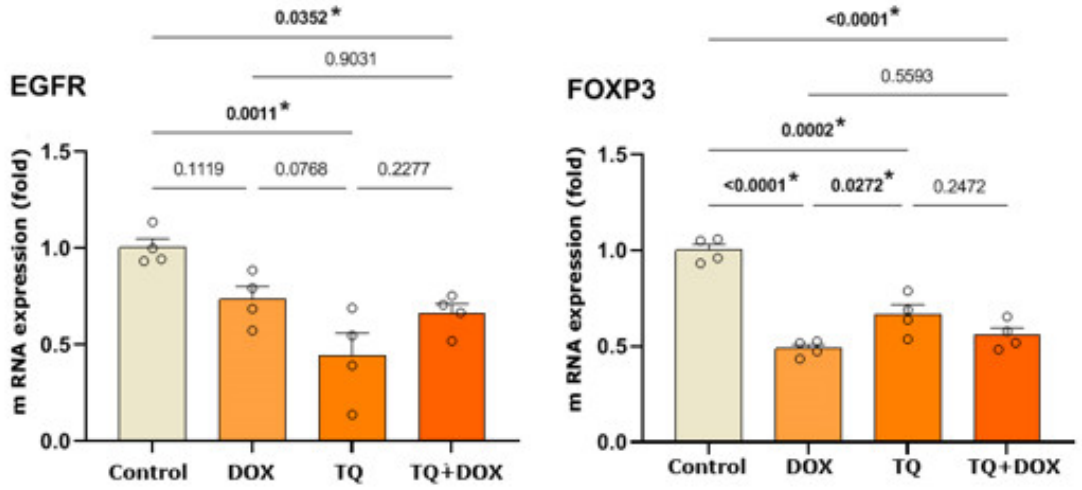

Figure 6. Relative fold increase values of EGFR and FOXP3 gene expressions 48 hours after single and combined drug administration (data normalized with β-actin and GAPDH mRNA level by multiple control method, n=4 data mean±SH), * means are statistically different.

3.3. Western Blot Analysis

The inhibitory effect of TQ and DOX on apoptosis and cell proliferation was analyzed at the protein level. As described in Figure 7, p-EGFR and protein expression of EGFR and FOXP3 were found to be significantly inhibited by 72-h IC50 TQ and DOX treatment (Figure 7).

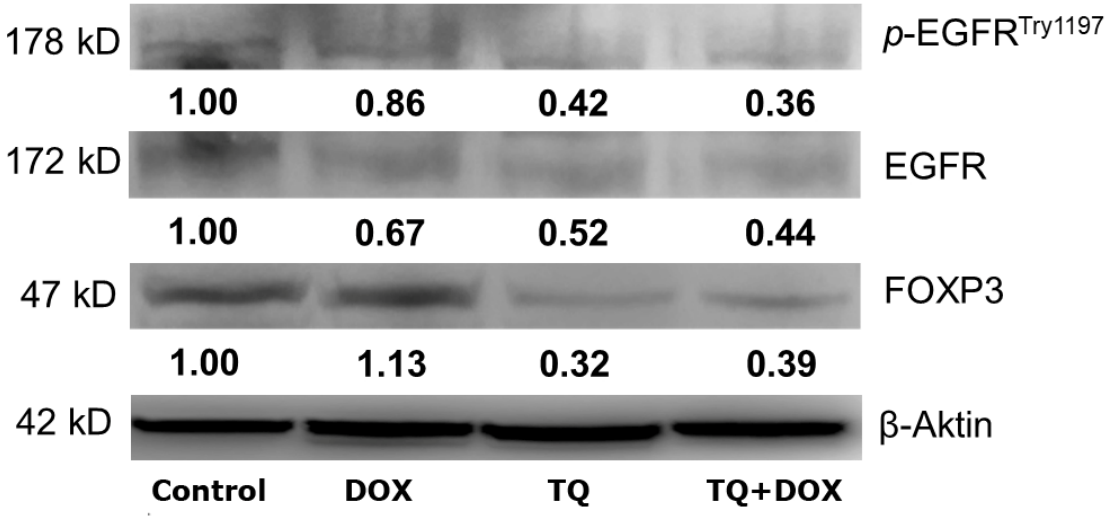

 doi:10.20944/preprints202407.2359.v1

Figure 7. p_EGFR, EGFR and FOXP3 protein levels in OVCAR-3 cell populations treated for 48 hours with IC50 doses of therapeutic agents.

3.4. PPI Analysis

Predictions from STRING analysis were used to depict protein interactions. The visualization showed 11 nodes and 46 edges (Figure 8). Based on nodal degree, the following genes were identified as the top 10 central genes: DCN, CDH1, ERBB2, ERBB3, EGF, CBL, PIK3CA, EREG, GAB1, HBEGF. These targets are hypothesized to be the primary targets in ovarian cancer of TQ.

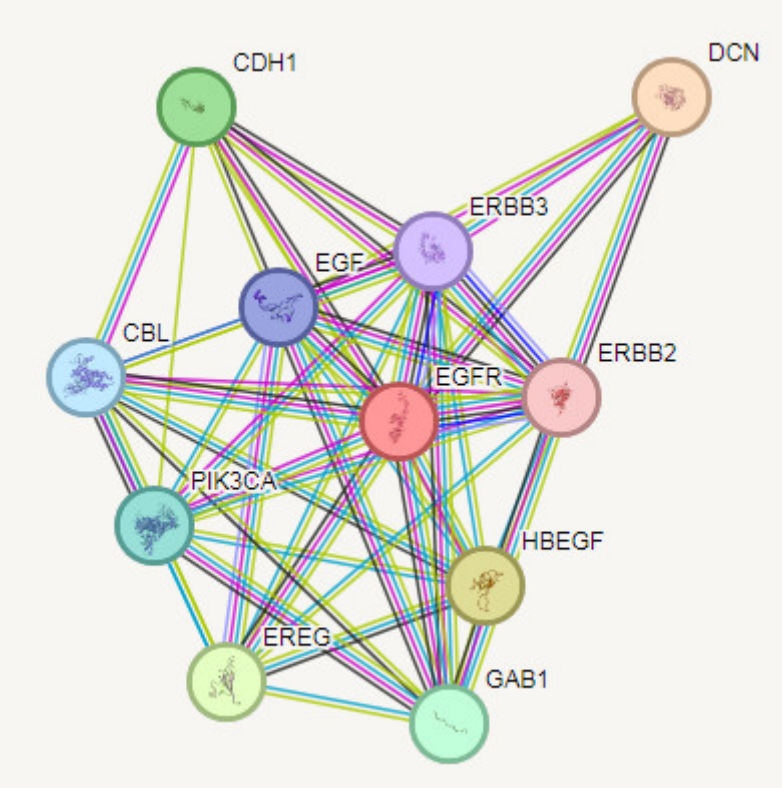

Figure 8. PPI and interaction between various genes of ovarian cancer.

3.5. KEGG Pathway Enrichment Analysis

KEGG pathway enrichment analysis of target genes was performed with Shiny 0.80 program. The findings showed that 72 genes were involved in the enrichment process and 50 pathways were cancer-related, exhibiting a significant correlation with target genes ($p < 0.05$). Basically ErbB signaling pathway EGFR tyrosine kinase inbitor resistance, Renal cell carcinoma, endometrial cancer ects. are shown (Figure 10).

Preprints.org (www.preprints.org) | NOT PEER-REVIEWED | Posted: 30 July 2024 doi:10.20944/preprints202407.2359.v1

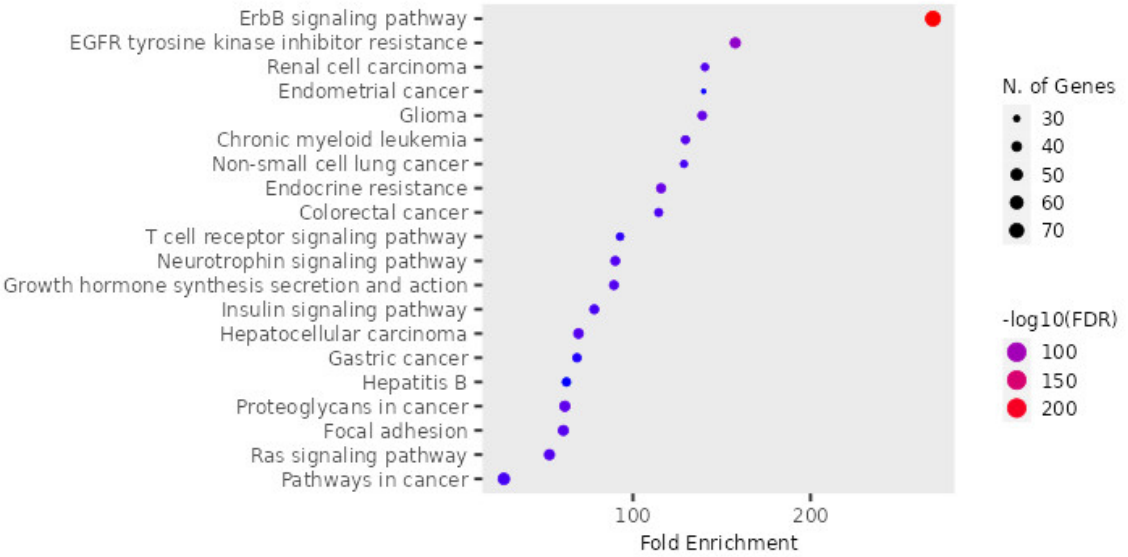

Figure 9. Enrichment analysis for the 72 common compound targets.

3.6. GO Functional Enrichment Analysis

Analysis findings show only important functions (Figure 10). Target genes were found to be involved in various cellular components in the BP category, such as ERBB2-EGFR signalin pathway. In terms of cellular components, target genes have been implicated in the Neuroglin receptor activity, EGFR activity etc.. It was found that the MF category exhibited roles such as ERBB3-ERBB2 complex, fotilin complex (Figure 10).

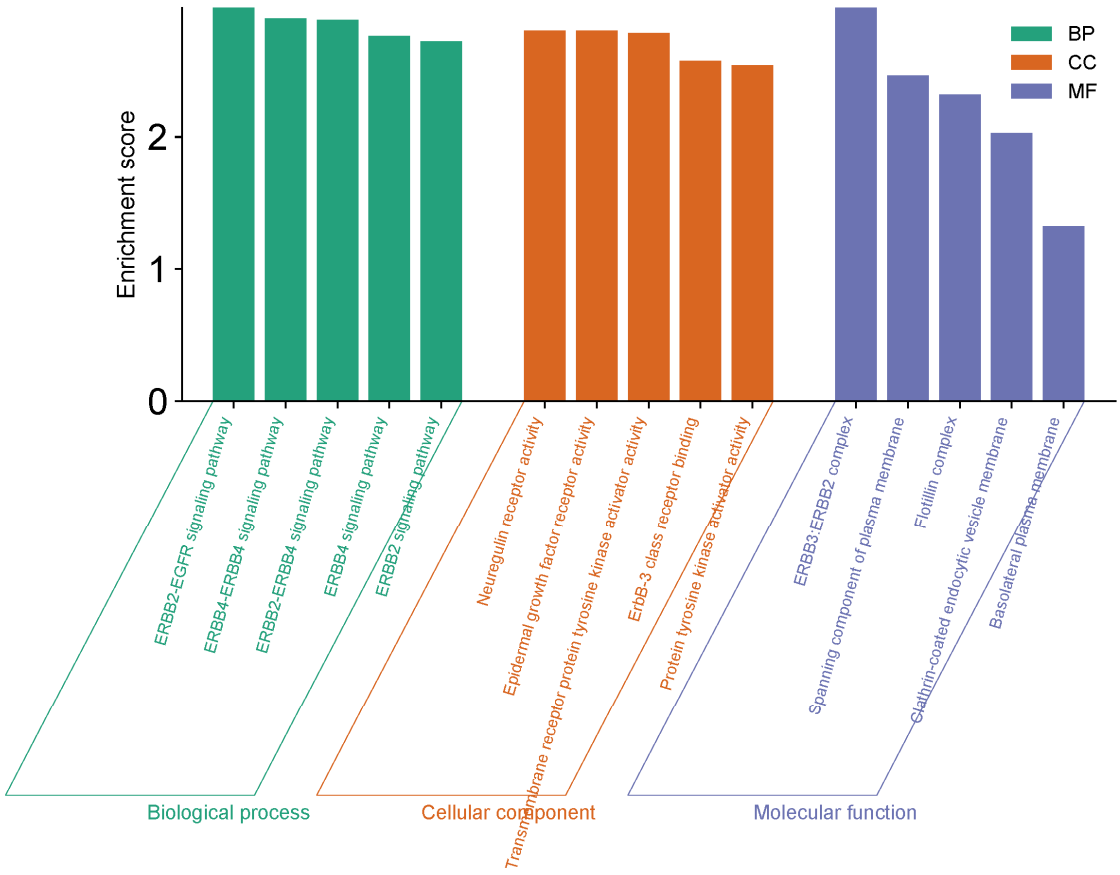

Figure 10. GO (Biological process, molecular function, and cellular component) analysis.

 doi:10.20944/preprints202407.2359.v1

4. Discussion

The underlying mechanisms that can lead to the formation and development of various types of cancer are completely different and often not fully understood. However, changes in genetic and epigenetic regulatory pathways are perceived as possible causes of the emergence of many types of cancer [14]. Accordingly, depending on the type and development of different cancers, various practical approaches have been applied for cancer treatment, including surgery, chemical drugs, radiation, immunological, targeting non-coding RNAs, and hormone therapies [15]. Despite the developments in traditional cancer treatment platforms, clinical applications have not been significantly effective due to disadvantages such as low durability of primary treatment, high probability of recurrence, serious side effects through general toxicity, insufficient selectivity and low quality of life [16]. Therefore, the search for modern curative procedures to combat various types of cancer with the least possible negative effects has become the focus of attention in recent years. Today, extensive research is being conducted on the anticancer properties of herbal bioactive compounds as revolutionary therapeutic agents thanks to their low toxicity, availability and affordable costs. Accordingly, one of the most promising and promising natural pharmaceuticals is thymoquinone. New studies have shown that regulation of microRNA (miRNA) expression through TQ has been accepted as a new technique in the fight against cancer [17]. Many studies on TQ have revealed that it has a beneficial therapeutic potential on human health, especially on cancer. There is a broad consensus in cancer research that TQ has promising anticancer activity in in vitro and in vivo model studies [18]. It has proven effective against a variety of cancer cell lines, where classical hallmarks of apoptosis such as chromatin condensation, translocation of phosphatidyl serine across the plasma membrane, and DNA fragmentation have been documented in TQ-treated cells [19]. The development of multidrug-resistant human tumor cells, including doxorubicin-resistant breast cancer cells, led to further research with TQ to evaluate its effectiveness against these types of cells [20]. Arafa et al. examined the anticancer effect of TQ in doxorubicin-resistant human breast cancer cells (MCF-7/DOX cells), revealing that it is significantly therapeutic in breast cancer cells [21]. Some studies have investigated whether TQ will regulate cell proliferation and apoptosis in MCF-7/DOX cells and its anticancer effect. The proposed mechanism is that TQ induces apoptosis in doxorubicin-resistant breast cancer cells through upregulation of phosphatase and tensin homolog (PTEN) at the transcriptional level. According to studies, doxorubicin (Dox) is one of the most powerful chemotherapeutic agents and is widely used in many cancer treatments. It acts as an anti-cancer, especially breast cancer and ovarian cancer. Additionally, dox can directly kill tumor cells through DNA damage [22], and studies show that it induces apoptosis in cancer cells through the activation of reactive oxygen species and p53 proteins [23]. N. sativa seed oil is reported to have many medicinal benefits. It contains especially fixed oils, volatile oils, proteins, alkaloids, coumarins, saponins, minerals, carbohydrates, fiber and water [24]. It has been reported that thymoquinone (TQ) inhibits the proliferation of many tumor cells such as colorectal carcinoma, breast adenocarcinoma, osteosarcoma, ovarian carcinoma, myeloblastic leukemia, pancreatic carcinoma and brain tumor [25].

A recent study reported that TQ exerts an antitumor effect through disruption of pro-survival mitogen-activated protein kinase kinase 7-mitogen-activated protein kinase 1 signaling in colorectal cancer. TQ showed a direct antitumor effect and also sensitized cancer cells to other treatments [26]. Velho-Pereira et al. [27] reported that TQ could radiosensitize human breast carcinoma cells. Jafri et al. [28] stated that TQ treatment in lung cancer could overcome resistance and sensitize lung cancer cells to CisPt. TQ (6 μg/mL) reduced the permeability of the plasma and mitochondrial membrane in the Caov-3 ovarian cancer cell line and increases apoptosis in ovarian cancer by reducing the nuclear area with a remarkable inhibition of both Bcl-2 and Bax, as well as inducing oxidative stress [29]. Another study showed that the combination of TQ with cisplatin led to better results when used separately, with a higher rate of apoptosis and Bax/Bcl-2 ratio [30]. Johnson et al. In 2019, they emphasized the importance of studying the structure-activity of TQ [31]. TQ-cisplatin combination increased DNA fragmentation and apoptosis and decreased proliferation [32]. Shoieb et al. found that TQ induced apoptosis in osteosarcoma cells and also reduced the number of cells in S phase.

 doi:10.20944/preprints202407.2359.v1

EGFR expression is also increased in ovarian cancer, and high expression is associated with poor prognosis (221). Western blot evaluation of a study revealed that bufalin reduced the total protein and phosphorylation levels of EGFR, and the phosphorylation levels of downstream molecules of EGFR, AKT, and ERK were downregulated under 200 nmol/L bufalin stimulation (222). EGF binds to the extracellular domain of EGFR and induces EGFR dimerization (223). Amplification or high expression of EGFRs in ovarian cancer plays a role in disease progression and prognosis (221). In a study, it was proven that Bufalin could inhibit the proliferation of ovarian cancer cells by binding to EGFR through molecular docking, and it was confirmed by western blot that bufalin could inhibit the proliferation of ovarian cancer cells through the EGFR/AKT/ERK pathway (222). However, Kang et al. (224) and Jiang et al. (225) studies show that bufalin inhibits the phosphorylation of EGFR protein only in lung cancer cells without affecting the level of total EGFR protein.

5. Conclusion

It was shown by qRT-PCR and western blot results that TQ and DOX can provide active treatment options on EGFR and FOXP3 signaling pathways. It has been suggested that TQ may modulate chemical mutogenicity, so it is necessary to determine its mechanisms and conditions through further studies. Thus, this active ingredient can be applied as a treatment adjuvant against increased oxidative stress and inflammation in chemotherapy.

Funding: None

Informed Consent Statement: Not Applicable

Data Availability Statement: All data supporting the findings of this study are available in public database from PubChem, STRING and within the paper.

Acknowledgments: This study is derived from İlhan Özdemir's doctoral thesis.

Conflicts of Interest: The authors declare that they have no competing interests.

References

1. Siegel RL, Miller KD, Jemal A. Cancer statistics, 2019. CA Cancer J Clin. 2019 Jan;69(1):7-34. doi: 10.3322/caac.21551.
2. Moufarrij S, Dandapani M, Arthofer E, Gomez S, Srivastava A, Lopez-Acevedo M, Villagra A, Chiappinelli KB. Epigenetic therapy for ovarian cancer: promise and progress. Clin Epigenetics. 2019 Jan 15;11(1):7. doi: 10.1186/s13148-018-0602-0.
3. Chauhan SC, Kumar D, Jaggi M. Mucins in ovarian cancer diagnosis and therapy. J Ovarian Res. 2009;2:21.
4. Bakhtiari H, Gheysarzadeh A, Ghanadian M, Aghaei M. 15-Hydroxy-8(17),13(E)-labdadiene-19-carboxylic acid (HLCA) inhibits proliferation and induces cell cycle arrest and apoptosis in ovarian cancer cells. Life Sci. 2021 Feb 15;267:118981. doi: 10.1016/j.lfs.2020.118981.
5. Llueca A, Ibañez MV, Cascales P, Gil-Moreno A, Bebia V, Ponce J, Fernandez S, Arjona-Sanchez A, Muruzabal JC, Veiga N, Diaz-Feijoo B, Celada C, Gilabert-Estelles J, Aghababyan C, Lacueva J, Calero A, Segura JJ, Maiocchi K, Llorca S, Villarin A, Climent MT, Delgado K, Serra A, Gomez-Quiles L, Llueca M, On Behalf Of Spain Gog And Gecop Working Group. Neoadjuvant Chemotherapy plus Interval Cytoreductive Surgery with or without Hyperthermic Intraperitoneal Chemotherapy (NIHIPEC) in the Treatment of Advanced Ovarian Cancer: A Multicentric Propensity Score Study. Cancers (Basel). 2023 Aug 26;15(17):4271. doi: 10.3390/cancers15174271.
6. Hong L, Wang X, Zheng L, Wang S, Zhu G. Tumor-associated macrophages promote cisplatin resistance in ovarian cancer cells by enhancing WTAP-mediated N6-methyladenosine RNA methylation via the CXCL16/CXCR6 axis. Cancer Chemother Pharmacol. 2023 Jul;92(1):71-81. doi: 10.1007/s00280-023-04533-8.
7. Jafari SM, Nazri A, Shabani M, Balajam NZ, Aghaei M. Galectin-9 induces apoptosis in OVCAR-3 ovarian cancer cell through mitochondrial pathway. Res Pharm Sci. 2018;13(6):557-65.
8. Raoufi-Nejad K, Javadi M, Torkamandi H, Rajabi M, Moeini A, Khanavi M, et al. Adverse drug reactions of herbal medicines during pregnancy amongst Iranian women. Res Pharm Sci. 2012;7(5):980.
9. Almatroodi SA, Almatroudi A, Alsahli MA, Khan AA, Rahmani AH. Thymoquinone, an Active Compound of Nigella sativa: Role in Prevention and Treatment of Cancer. Curr Pharm Biotechnol. 2020;21(11):1028-1041. doi: 10.2174/1389201021666200416092743.

10. Mehner C, Oberg AL, Goergen KM, Kalli KR, Maurer MJ, Nassar A, Goode EL, Keeney GL, Jatoi A, Radisky DC, Radisky ES. EGFR as a prognostic biomarker and therapeutic target in ovarian cancer: evaluation of patient cohort and literature review. Genes Cancer. 2017 May;8(5-6):589-599. doi: 10.18632/genesandcancer.142.
11. Gelatti ACZ, Drilon A, Santini FC. Optimizing the sequencing of tyrosine kinase inhibitors (TKIs) in epidermal growth factor receptor (EGFR) mutation-positive non-small cell lung cancer (NSCLC). Lung Cancer. 2019 Nov;137:113-122. doi: 10.1016/j.lungcan.2019.09.017.
12. Teplinsky E, Muggia F. EGFR and HER2: is there a role in ovarian cancer? Translational Cancer Research. 2015;4:10.
13. Rendell A, Thomas-Bland I, McCuish L, Taylor C, Binju M, Yu Y. Targeting Tyrosine Kinases in Ovarian Cancer: Small Molecule Inhibitor and Monoclonal Antibody, Where Are We Now? Biomedicines. 2022 Aug 29;10(9):2113. doi: 10.3390/biomedicines10092113.
14. Parreno V, Loubiere V, Schuettengruber B, Fritsch L, Rawal CC, Erokhin M, Győrffy B, Normanno D, Di Stefano M, Moreaux J, Butova NL, Chiolo I, Chetverina D, Martinez AM, Cavalli G. Transient loss of Polycomb components induces an epigenetic cancer fate. Nature. 2024 May;629(8012):688-696. doi: 10.1038/s41586-024-07328-w.
15. Tajan M, Vousden KH. Dietary Approaches to Cancer Therapy. Cancer Cell. 2020 Jun 8;37(6):767-785. doi: 10.1016/j.ccell.2020.04.005.
16. Mohammadabadi M, Mozafari M. Enhanced efficacy and bioavailability of thymoquinone using nanoliposomal dosage form. J Drug Deliv Sci Technol. 2018;47:445-53.
17. Khan MA, Tania M, Fu J. Epigenetic role of thymoquinone: impact on cellular mechanism and cancer therapeutics. Drug Discov Today. 2019;24(12):2315-22.
18. Attoub S, Sperandio O, Raza H, Arafat K, Al-Salam S, Al Sultan MA, et al. Thymoquinone as an anticancer agent: evidence from inhibition of cancer cells viability and invasion in vitro and tumor growth in vivo. Fundam Clin Pharmacol. 2013;27(5):557-69.
19. Alam M, Hasan GM, Ansari MM, Sharma R, Yadav DK, Hassan MI. Therapeutic implications and clinical manifestations of thymoquinone. Phytochemistry. 2022 Aug;200:113213. doi: 10.1016/j.phytochem.2022.113213.
20. Gholamnezhad Z, Rafatpanah H, Sadeghnia HR, Boskabady MH. Immunomodulatory and cytotoxic effects of Nigella sativa and thymoquinone on rat splenocytes. Food Chem Toxicol. 2015 Dec;86:72-80. doi: 10.1016/j.fct.2015.08.028.
21. Arafa el SA, Zhu Q, Shah ZI, Wani G, Barakat BM, Racoma I, et al. Thymoquinone up-regulates PTEN expression and induces apoptosis in doxorubicin-resistant human breast cancer cells. Mutat Res. 2011;706(1-2):28-35.
22. Li ZL, Chen C, Yang Y, Wang C, Yang T, Yang X, et al. Gamma secretase inhibitor enhances sensitivity to doxorubicin in MDA-MB-231 cells. Int J Clin Exp Pathol. 2015;8(5):4378-87.
23. Wang S, Konorev EA, Kotamraju S, Joseph J, Kalivendi S, Kalyanaraman B. Doxorubicin induces apoptosis in normal and tumor cells via distinctly different mechanisms. intermediacy of H(2)O(2)- and p53-dependent pathways. J Biol Chem. 2004;279(24):25535-43.
24. Ijaz H, Tulain UR, Qureshi J, Danish Z, Musayab S, Akhtar MF, Saleem A, Khan KK, Zaman M, Waheed I, Khan I, Abdel-Daim M. Review: Nigella sativa (Prophetic Medicine): A Review. Pak J Pharm Sci. 2017 Jan;30(1):229-234.
25. Ashour AE, Ahmed AF, Kumar A, Zoheir KM, Aboul-Soud MA, Ahmad SF, et al. Thymoquinone inhibits growth of human medulloblastoma cells by inducing oxidative stress and caspase-dependent apoptosis while suppressing NF-κB signaling and IL-8 expression. Mol Cell Biochem. 2016;416(1-2):141-55.
26. Housman G, Byler S, Heerboth S, Lapinska K, Longacre M, Snyder N, et al. Drug resistance in cancer: an overview. Cancers (Basel). 2014;6(3):1769-92.
27. Velho-Pereira R, Kumar A, Pandey BN, Jagtap AG, Mishra KP. Radiosensitization in human breast carcinoma cells by thymoquinone: role of cell cycle and apoptosis. Cell Biol Int. 2011 Oct;35(10):1025-9. doi: 10.1042/CBI20100701.
28. Jafri SH, Glass J, Shi R, Zhang S, Prince M, Kleiner-Hancock H. Thymoquinone and cisplatin as a therapeutic combination in lung cancer: In vitro and in vivo. J Exp Clin Cancer Res. 2010 Jul 1;29(1):87. doi: 10.1186/1756-9966-29-87.
29. Taha MM, Sheikh BY, Salim LZ, Mohan S, Khan A, Kamalidehghan B, et al. Thymoquinone induces apoptosis and increase ROS in ovarian cancer cell line. Cell Mol Biol (Noisy-le-grand). 2016;62(6):97-101.
30. Liu X, Dong J, Cai W, Pan Y, Li R, Li B. The Effect of Thymoquinone on Apoptosis of SK-OV-3 Ovarian Cancer Cell by Regulation of Bcl-2 and Bax. Int J Gynecol Cancer. 2017;27(8):1596-601.
31. Johnson-Ajinwo OR, Ullah I, Mbye H, Richardson A, Horrocks P, Li WW. The synthesis and evaluation of thymoquinone analogues as anti-ovarian cancer and antimalarial agents. Bioorg Med Chem Lett. 2018;28(7):1219-22.

 doi:10.20944/preprints202407.2359.v1

32. Bonello M, Sims AH, Langdon SP. Human epidermal growth factor receptor targeted inhibitors for the treatment of ovarian cancer. Cancer Biol Med. 2018;15(4):375-88.
33. Dou L, Zou D, Song F, Jin Y, Li Y, Zhang Y. Bufalin suppresses ovarian cancer cell proliferation via EGFR pathway. Chin Med J (Engl). 2021;135(4):456-61.
34. Shen LS, Jin XY, Wang XM, Tou LZ, Huang J. Advances in endocrine and targeted therapy for hormone-receptor-positive, human epidermal growth factor receptor 2-negative advanced breast cancer. Chin Med J (Engl). 2020;133(9):1099-108.
35. Kang XH, Xu ZY, Gong YB, Wang LF, Wang ZQ, Xu L, et al. Bufalin Reverses HGF-Induced Resistance to EGFR-TKIs in EGFR Mutant Lung Cancer Cells via Blockage of Met/PI3k/Akt Pathway and Induction of Apoptosis. Evid Based Complement Alternat Med. 2013;2013:243859.
36. Jiang Y, Zhang Y, Luan J, Duan H, Zhang F, Yagasaki K, et al. Effects of bufalin on the proliferation of human lung cancer cells and its molecular mechanisms of action. Cytotechnology. 2010;62(6):573-83.